Effective Guided Image Filtering for Contrast Enhancement

Zongwei Lu, Bangyuan Long, Kang Li, and Fajin Lu

***Abstract*—Although the guided image filtering (GIF) has an excellent edge-preserving property, it is prone to suffer from the halo artifacts near the edges. Weighted GIF and gradient-domain GIF try to address the problem by incorporating an edge-aware weighting into GIF. However, they are very sensitive to the regularization parameter and the halo artifacts will become serious as the regularization parameter increases. Moreover, noise in the background is often amplified because of the fixed amplification factor for the detail layer. In this letter, an effective GIF is proposed for better contrast enhancement. First, the average of local variances for all pixels is incorporated into the cost function of GIF for preserving the edges accurately in the base layer. Second, the amplification factor for the detail layer is calculated in a content-adaptive way for suppressing the noise while boosting the fine details. Experimental results show that the proposed filter is more robust to the regularization parameter and can produce visually pleasing output images. Compared to GIF and its related filters, halo artifacts and noise are reduced or attenuated by the proposed filter significantly.**

***Index Terms*—Contrast enhancement, detail enhancement, edge-preserving, guided image filtering (GIF).**

I. Introduction

THE edge-preserving smoothing techniques have many applications in image processing and computer vision, including contrast enhancement [1], tone mapping of high dynamic range images [2], structure extraction from texture [3], fusion of differently exposed images [4], and single image haze removal [5]. Often, the edge-preserving smoothing techniques decompose an image into a piecewise smooth base layer with large-scale variations in intensity and a detail layer with small-scale details such as noise or texture. By amplifying the detail layer, a detail enhanced image is produced.

Edge-preserving smoothing techniques can be categorized into two groups: global and local filters. The global filters are often based on the optimized performance criterion, consisting of a data term and a regularization term. With different data terms and regularization terms, many global filters have been proposed [6]–[8]. While the global filters always produce better results, they have high computational cost. On the contrary, the local filters are quite simpler [9]–[11]. However, because the local filters cannot preserve the edges well as global filters, halo artifacts are prone to be produced near the edges in the resultant images, which is usually not favored for image processing and computer vision. As pointed out in [12] and [13], one of the reasons for halo artifacts may lie in the constant of the regularization parameter. Moreover, because the amplification factor for the detail layer is fixed, when local filters are applied for contrast enhancement, noise in the background will be amplified and the visual quality of the output images will be degraded.

Guided image filtering (GIF) is a well-known local filter for its excellent edge-preserving property and high efficiency [11]. Considering the structure of the guided image, GIF uses a linear model to compute the pixel values in a window. Because the regularization parameter in the GIF is fixed, halo artifacts will be inevitably produced for strong edges in the output images. In order to reduce or attenuate the halo artifacts, weighted GIF (WGIF) [14] calculates the local variances of 3×3 windows of all pixels as the edge-aware weighting and preserves the edges better than GIF. Later, gradient-domain GIF (GGIF) [15] extends the WGIF by including the local variances of the windows for the filter size. While WGIF and GGIF can preserve the edges more accurately than GIF, they are very sensitive to the regularization parameter and the halo artifacts will become serious with the increase of the regularization parameter.

In the following, GIF and its related works are introduced in Section II. The proposed filter, effective GIF (EGIF), is presented in Section III. Experimental results are shown in Section IV. Finally, some conclusions are given in Section V.

II. GIF and Related Works

In GIF, the filter output q is a linear transform of a guided image I in a window ω_k centered at the pixel k [11]

$$q_i = a_k I_i + b_k \quad \forall i \in \omega_k \tag{1}$$

where i and k are the indices, and (a_k, b_k) are two constants in the window. Their values are obtained by minimizing a cost function defined as

$$E(a_k, b_k) = \min \sum_{i \in \omega_k} \left((a_k I_i + b_k - p_i)^2 + \lambda a_k^2 \right) \tag{2}$$

Manuscript received July 5, 2018; revised August 16, 2018; accepted August 22, 2018. Date of publication August 30, 2018; date of current version September 13, 2018. This work was supported in part by the Municipal Health and Family Planning Commission, Chongqing, China, under Grant 2016MSXM065. The associate editor coordinating the review of this manuscript and approving it for publication was Dr. Daniel P. K. Lun. *(Corresponding author: Bangyuan Long.)*

Z. Lu is with the State Key Laboratory of Power Transmission Equipment and System Security and New Technology, Chongqing University, Chongqing 400030, China (e-mail: luzongwei@hotmail.com).

B. Long and K. Li are with the Department of Radiology, General Hospital of Chongqing, Chongqing 400013, China (e-mail: bangyuanl@hotmail.com; kangli@hotmail.com).

F. Lu is with the Department of Radiology, First Affiliated Hospital of Chongqing Medical University, Chongqing 400016, China (e-mail: fjlu0@sina.com).

Color versions of one or more of the figures in this letter are available online at http://ieeexplore.ieee.org.

Digital Object Identifier 10.1109/LSP.2018.2867896

This work is licensed under a Creative Commons Attribution 3.0 License. For more information, see http://creativecommons.org/licenses/by/3.0/

where λ is a regularization parameter penalizing large a_k and p is the filter input.

The optimal values for (a_k, b_k) are calculated as

$$a_k = \frac{\frac{1}{|\omega|}\sum_{i\in\omega_k} I_i p_i - \mu_k \bar{p}_k}{\sigma_k^2 + \lambda} \tag{3}$$

$$b_k = \bar{p}_k - a_k \mu_k \tag{4}$$

where μ_k and σ_k^2 are the mean and variance of I in ω_k, $|\omega|$ is the number of pixels in ω_k, and $\bar{p}_k$ is the mean of p in ω_k.

The parameter λ decides the criterion of a "flat patch" or a "high variance." More specifically, the patches with variance (σ_k^2) much smaller than λ are smoothed, whereas those with variance much larger than λ are preserved [11]. The role of λ will inspire a new weighting proposed in Section III-A.

In order to preserve the edges better, WGIF incorporates an edge-aware weighting into (2) [14] as

$$E(a_k, b_k) = \min \sum_{i\in\Omega_{G,\xi_1}} \left((a_k I_i + b_k - p_i)^2 + \frac{\lambda}{\Gamma_G(p')} a_k^2\right) \tag{5}$$

where $\Gamma_G(p')$ is the edge-aware weighting and is calculated by using local variances of 3×3 windows of all pixels as follows:

$$\Gamma_G(p') = \frac{1}{N}\sum_{p=1}^{N} \frac{\sigma_{G,1}^2(p')}{\sigma_{G,1}^2(p)} \tag{6}$$

where $\sigma_{G,1}^2(p')$ is the variance of I in the window $\Omega_{G,1}(p')$, and N is the number of pixels in the guided image I.

Considering the local variances of the windows for the filter size, GGIF defines edge-aware weighting as follows [15]:

$$\Gamma_G(p') = \frac{1}{N}\sum_{p=1}^{N} \frac{\chi(p')}{\chi(p)} \tag{7}$$

where $\chi(p') = \sigma_{G,1}(p')\sigma_{G,\zeta_1}(p')$, $\sigma_{G,\zeta_1}^2(p')$ is the variance of I in the window $\Omega_{G,\xi_1}(p')$, and ξ_1 is the window size of the filter.

While both WGIF and GGIF can preserve the edges more accurately than GIF theoretically, experimental results show that the halo artifacts cannot be avoided for strong edges when they are applied for contrast enhancement. Based on (3), decreasing the parameter λ can definitely reduce the halo artifacts, otherwise the resultant image will become close to the input image.

III. Proposed Filtering

In the following, a new weighting is incorporated into the cost function of the GIF to preserve the edges accurately and a content-adaptive amplification factor is presented to reduce the noise in the background.

A. New Weighting

The average of local variances for all pixels is defined as

$$\Gamma = \bar{\sigma}^2 = \frac{1}{N}\sum_{k=1}^{N} \sigma_k^2 \tag{8}$$

where σ_k^2 is the local variance of I in ω_k.

Inspired by the role of λ in Section II, (8) is incorporated into (2) as

$$E(a_k, b_k) = \min \sum_{i\in\omega_k} \left((a_k I_i + b_k - p_i)^2 + \lambda\Gamma a_k^2\right). \tag{9}$$

The optimal value for a_k is calculated as follows and b_k is unchanged according to (4):

$$a_k = \frac{\frac{1}{|\omega|}\sum_{i\in\omega_k} I_i p_i - \mu_k \bar{p}_k}{\sigma_k^2 + \lambda\Gamma}. \tag{10}$$

When GIF is applied for contrast enhancement, I and p are identical and the following equations hold:

$$\frac{1}{|\omega|}\sum_{i\in\omega_k} I_i p_i - \mu_k \bar{p}_k = \sigma_k^2 \tag{11}$$

$$\bar{p}_k = \mu_k. \tag{12}$$

Substituting (11) and (12) into (10) and (4), respectively, we will get

$$a_k = \frac{\sigma_k^2}{\sigma_k^2 + \lambda\Gamma} \tag{13}$$

$$b_k = (1 - a_k)\mu_k. \tag{14}$$

The numerator and denominator in (13) are divided by σ_k^2, respectively, as

$$a_k = \frac{1}{1 + \lambda\frac{\Gamma}{\sigma_k^2}} = \frac{1}{1 + \lambda\frac{\bar{\sigma}^2}{\sigma_k^2}}. \tag{15}$$

If a pixel is in the middle of a "high-variance" area, its local variance should be greater than average variance. According to (14) and (15), a_k and b_k become close to 1 and 0, respectively, and the value of the pixel is unchanged. On the other side, if a pixel is in the middle of a "flat patch" area, its local variance should be less than the average variance. a_k and b_k become close to 0 and 1, respectively, and the value of the pixel is the average of the pixels nearby.

After computing (a_k, b_k) for all patches ω_k in the image, the filter output is computed as follows [11]:

$$q_i = \frac{1}{|\omega|}\sum_{k:i\in\omega_k} (a_k I_i + b_k) = \bar{a}_i I_i + \bar{b}_i \tag{16}$$

where $\bar{a}_i = \frac{1}{|\omega|}\sum_{k\in\omega_i} a_k$ and $\bar{b}_i = \frac{1}{|\omega|}\sum_{k\in\omega_i} b_k$.

Although WGIF can produce a larger value of a_k for the pixel on the edge, the values of a_k for pixels adjacent to the edge are smaller. So, the value of $\bar{a}_i$ will become small. On the other side, EGIF can produce larger values of a_k for pixels both adjacent to and on the edge, hence the value of $\bar{a}_i$ is large. The same holds for $\bar{b}_i$.

Fig. 2(a) is a synthetic image. One-dimensional illustrations of the GIF, WGIF, GGIF, and EGIF with different values of λ for Fig. 2(a) are shown in Fig. 1(a)–(c).

As shown in Fig. 1(a)–(c), the proposed filter EGIF preserves the edges more accurately than the GIF, WGIF, and GGIF. The output values of the proposed filter are almost the same as the input values near the edges, whereas the output values of the GIF, WGIF, and the GGIF are far away from the input values. As the value of λ increases, GIF, WGIF, and GGIF cannot preserve the edges accurately and the halo artifacts will become serious, whereas EGIF is more robust to the value of λ.

Fig. 2(b)–(e) shows the base layers produced by the GIF, WGIF, GGIF, and EGIF for the synthetic image shown in Fig. 2(a), respectively. It is seen from Fig. 2 that GIF, WGIF, and GGIF cannot preserve the edges accurately and the halo

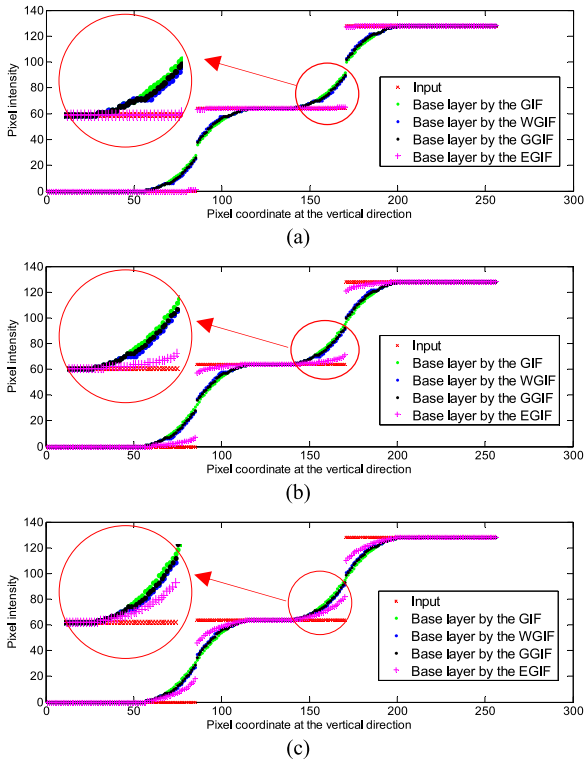

Fig. 1. One-dimensional illustrations of the GIF, WGIF, GGIF, and EGIF. (a) $\zeta 1 = 16$, $\lambda = 0.1$. (b) $\zeta 1 = 16$, $\lambda = 1$. (c) $\zeta 1 = 16$, $\lambda = 5$.

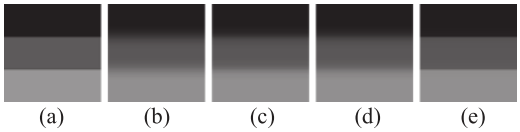

Fig. 2. (a) Input image. Base layer produced by (b) GIF, (c) WGIF, (d) GGIF, and (e) EGIF. $\zeta 1 = 16$, $\lambda = 1$ in all the four filters.

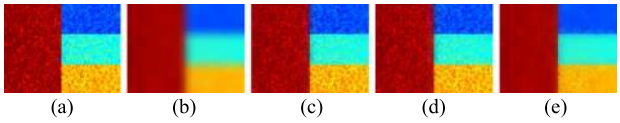

Fig. 3. (a) Noise image. Base layer produced by (b) GIF, (c) WGIF, (d) GGIF, and (e) EGIF. $\zeta 1 = 16$, $\lambda = 5$ in all the four filters.

artifacts are produced near the edges. By comparison, EGIF preserves the edges more accurately than the GIF, WGIF, and GGIF and the halo artifacts are not noticeable near the edges. This demonstrates clearly that the new weighting proposed is very effective for preserving the edges accurately.

On the other side, EGIF can smooth flat areas better than WGIF and GGIF when λ is large. Fig. 3(a) is an example from [8]. Fig. 3(b)–(e) shows the resultant images by the GIF, WGIF, GGIF, and EGIF, respectively. It can be seen clearly from Fig. 3 that EGIF smooths the flat area well while preserving the edges more accurately than GIF. In contrast, both WGIF and GGIF fail to smooth the flat area.

B. Content-Adaptive Amplification Factor

Mathematically, the detail layer r is defined as follows:

$$r = I - q \tag{17}$$

where q is the base layer and is defined in (16).

Multiplying the detail layer by an amplification factor β

$$r' = \beta \cdot r = \beta \cdot (I - q) \tag{18}$$

where r' is the enhanced detail layer. The value of β is fixed for GIF, WGIF, and GGIF ($\beta = 5$).

The output image f is the sum of q and r'

$$f = q + r'. \tag{19}$$

Substituting (16) into (18)

$$r' = \beta \cdot (I - \bar{a}I - \bar{b}) = \beta \cdot (1 - \bar{a})I - \beta \cdot \bar{b}. \tag{20}$$

The gradient of the enhanced detail layer is calculated as follows:

$$\nabla r' = \beta \cdot (1 - \bar{a}) \cdot \nabla I. \tag{21}$$

Based on (1), the gradient of the base layer is calculated as follows:

$$\nabla q = \bar{a} \cdot \nabla I. \tag{22}$$

Generally speaking, the gradient of the detail layer should not be bigger than the gradient of the base layer. Otherwise, the noise in the detail layer will be amplified. So, the following inequality holds:

$$\nabla r' \leq \nabla q. \tag{23}$$

Substituting (21) and (22) into (23)

$$\beta \cdot (1 - \bar{a}) \cdot \nabla I \leq \bar{a} \cdot \nabla I. \tag{24}$$

Then,

$$\beta \leq \frac{\bar{a}}{1 - \bar{a}}. \tag{25}$$

When the value of β is small, the details will be suppressed. On the other side, the noise will be amplified for a larger value of β. So, there is a tradeoff between noise suppression and fine details enhancement. In this letter, considering the balance between the noise suppression and detail enhancement, the value of β is set as follows:

$$\beta = \frac{\bar{a}}{1 - \bar{a}}. \tag{26}$$

Here, $\beta > 0$ since $0 < \bar{a} < 1$ based on (15) and (16).

If a pixel is in the middle of a "high-variance" area, $\bar{a}_k$ will become close to 1 based on (15) and (16). According to (26), the value of β will be larger to boost the pixel in the "high-variance" area. Similarly, if a pixel is in the middle of a "flat patch" area, $\bar{a}_k$ will become close to 0. Then, the value of β will be smaller to suppress the pixel in the "flat patch" area.

According to (26), the value of β will be very large when $\bar{a}_k$ becomes close to 1. So, it is possible that the image will be overenhanced near the edges. Thus, in order to avoid overenhancement, a coefficient γ is introduced into (26) as follows:

$$\beta = \left(\frac{\bar{a}}{1 - \bar{a}}\right)^{\gamma} \tag{27}$$

where $0 < \gamma \leq 1$. For simplicity, $\gamma = 1$ unless specified.

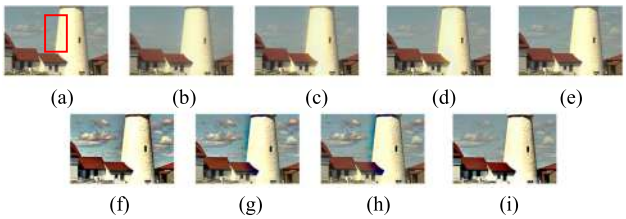

Fig. 4. (a) Input. Zoom-in patches for base layer by (b) GIF, (c) WGIF, (d) GGIF, and (e) EGIF. Enhanced by (f) GIF, (g) WGIF, (h) GGIF, and (i) EGIF.

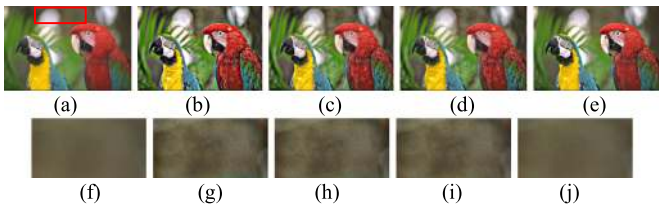

Fig. 5. (a) Input. Enhanced by (b) GIF, (c) WGIF, (d) GGIF, and (e) EGIF. (f)–(j) Zoom-in patches for Input, GIF, WGIF, GGIF, and EGIF.

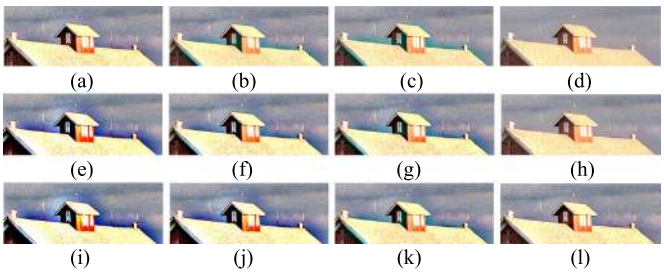

Fig. 6. From left to right: zoom-in patches for GIF, WGIF, GGIF, and EGIF. (a)–(d) $\zeta 1 = 16$, $\lambda = 0.01$. (e)–(h) $\zeta 1 = 16$, $\lambda = 0.1$. (i)–(l) $\zeta 1 = 16$, $\lambda = 1$.

IV. Experimental Results

The experiment is conducted in MATLAB R2013a on a PC with 2.60 GHz Intel Pentium Dual-Core Processor. $\lambda = 0.1^2$ and $\zeta_1 = 16$ are set for all four filters unless specified [11]. The amplification factor is 5 for GIF, WGIF, and GGIF. Images coming from Kodak [17], SIPI [18], CVG [19], and BSDS500 [20] are tested. The experimental results and code can also be found at http://sites.google.com/view/bangyuanl/.

Fig. 4(a) is the input image. Fig. 4(b)–(e) shows the base layers filtered by GIF, WGIF, GGIF, and EGIF. Fig. 4(f)–(i) shows the output images by GIF, WGIF, GGIF, and EGIF. GIF, WGIF, and GGIF produce weak halo artifacts for base layers and strong halo artifacts for output images. In contrast, EGIF does not produce halo artifacts for both base layer and output image.

As shown in Fig. 5(g)–(j), while GIF, WGIF, and GGIF do not produce the halo artifacts, noise in the background is amplified because of the fixed amplification factor. EGIF suppresses the noise since the amplification factor is calculated according to (25).

In order to compare the performance of edge-preserving for GIF, WGIF, GGIF, and EGIF fairly, the amplification factor for the detail layer is set as 5 for EGIF.

Fig. 6(a)–(d), (e)–(h), and (i)–(l) shows the zoom-in patches produced by GIF, WGIF, GGIF, and EGIF for different values of λ, respectively. It is clearly seen that the halo artifacts near the roof become serious for GIF, WGIF, and GGIF as the value of λ increases from 0.01 to 1, whereas EGIF does not produce obvious halo artifacts when the value of λ increases.

Fig. 7. (a) Input. (b) $\gamma = 0.5$. (c) $\gamma = 1$. (d) $\gamma = 1.5$. $\zeta 1 = 16$, $\lambda = 0.01$.

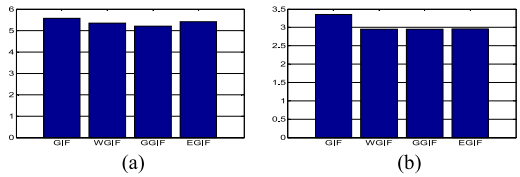

Fig. 8. (a) Average NIQMC for Kodak by different filters. (b) Average NIQE for Kodak by different filters.

Finally, Fig. 7(b)–(d) shows the output images produced by EGIF for different values of γ. Obviously, the image will be overenhanced when $\gamma > 1$.

The dataset Kodak having 24 natural images is chosen for objective assessment. The no-reference image quality metric for contrast enhancement (NIQMC) is utilized to evaluate the contrast enhancement quality [21]. Higher values represent better qualities of image contrast. The naturalness image quality evaluator (NIQE) is utilized to evaluate image quality blindly [22]. Lower values represent better qualities.

It can be seen from Fig. 8(a) that GIF has the highest average NIQMC value. EGIF has a higher average NIQMC value than both WGIF and GGIF. Although GIF has a higher average NIQMC value than EGIF, it is easy to overenhance images and produce the halo artifacts and noise, as shown in Figs. 4–6.

Fig. 8(b) indicates that WGIF, GGIF, and EGIF have almost the same average NIQE values. This indicates that the visual quality of the output images produced by the EGIF is comparable with WGIF and GGIF. Nevertheless, both WGIF and GGIF are prone to produce the halo artifacts near strong edges.

V. Conclusion

When GIF, WGIF, and GGIF are applied for contrast enhancement, they are prone to produce the halo artifacts near the strong edges and the noise in the background is amplified. The visual quality of output images will be degraded. The proposed filter, EGIF, overcomes these shortcomings by incorporating the average of local variances for all pixels into the GIF for preserving the edges more accurately in the base layer and calculating the amplification factor in a content-adaptive way for suppressing the noise and boosting the fine details in the detail layer. Compared with the GIF, WGIF, and GGIF, EGIF is more robust to the regularization parameter and can reduce or attenuate the halo artifacts and noise significantly. So, EGIF can produce the output images with higher visual quality.

REFERENCES

[1] R. Fattal, M. Agrawala, and S. Rusinkiewicz, "Multiscale shape and detail enhancement from multi-light image collections," *ACM Trans. Graph.*, vol. 26, no. 3, pp. 51:1–51:10, Aug. 2007.

[2] F. Durand and J. Dorsey, "Fast bilateral filtering for the display of high dynamic range images," *ACM Trans. Graph.*, vol. 21, no. 3, pp. 257–266, Jul. 2002.

[3] L. Xu, Q. Yan, Y. Xia, and J. Jia, "Structure extraction from texture via relative total variation," *ACM Trans. Graph.*, vol. 31, no. 6, Nov. 2012, Art. no. 139.

[4] Z. G. Li, J. H. Zheng, and S. Rahardja, "Detail-enhanced exposure fusion," *IEEE Trans. Image Process.*, vol. 21, no. 11, pp. 4672–4676, Nov. 2012.

[5] K. He, J. Sun, and X. Tang, "Single image haze removal using dark channel prior," *IEEE Trans. Pattern Anal. Mach. Intell.*, vol. 33, no. 12, pp. 2341–2353, Dec. 2011.

[6] L. I. Rudin, S. Osher, and E. Fatemi, "Nonlinear total variation based noise removal algorithms," *Phys. D, Nonlinear Phenomena*, vol. 60, no. 1–4, pp. 259–268, Nov. 1992.

[7] L. Xu, C. Lu, Y. Xu, and J. Jia, "Image smoothing via *L*0 gradient minimization," *ACM Trans. Graph.*, vol. 30, no. 6, Dec. 2011, Art. no. 174.

[8] Z. Farbman, R. Fattal, D. Lischinski, and R. Szeliski, "Edge-preserving decompositions for multiscale tone and detail manipulation," *ACM Trans. Graph.*, vol. 27, no. 3, pp. 249–256, Aug. 2008.

[9] C. Tomasi and R. Manduchi, "Bilateral filtering for gray and color images," in *Proc. IEEE Int. Conf. Comput. Vis.*, Jan. 1998, pp. 836–846.

[10] P. Choudhury and J. Tumblin, "The trilateral filter for high contrast images and meshes," in *Proc. Eurograph. Symp. Rendering*, 2003, pp. 186–196.

[11] K. He, J. Sun, and X. Tang, "Guided image filtering," *IEEE Trans. Pattern Anal. Mach. Learn.*, vol. 35, no. 6, pp. 1397–1409, Jun. 2013.

[12] B. Y. Zhang and J. P. Allebach, "Adaptive bilateral filter for sharpness enhancement and noise removal," *IEEE Trans. Image Process.*, vol. 17, no. 5, pp. 664–678, May 2008.

[13] Z. Li, J. Zheng, Z. Zhu, S. Wu, W. Yao, and S. Rahardja, "Content adaptive bilateral filtering," in *Proc. IEEE Int. Conf. Multimedia Expo.*, Jul. 2013, pp. 1–6.

[14] Z. Li, J. Zheng, Z. Zhu, W. Yao, and S. Wu, "Weighted guided image filtering," *IEEE Trans. Image Process.*, vol. 24, no. 1, pp. 120–129, Jan. 2015.

[15] F. Kou, W. Chen, C. Wen, and Z. Li, "Gradient domain guided image filtering," *IEEE Trans. Image Process.*, vol. 24, no. 11, pp. 4528–4539, Nov. 2015.

[16] Z. Wang, A. C. Bovik, H. R. Sheikh, and E. P. Simoncelli, "Image quality assessment: From error visibility to structural similarity," *IEEE Trans. Image Process.*, vol. 13, no. 4, pp. 600–612, Apr. 2004.

[17] 2013. [Online]. Available: http://r0k.us/graphics/kodak/

[18] 2018. [Online]. Available: http://sipi.usc.edu/database/

[19] 2014. [Online]. Available: http://decsai.ugr.es/cvg/dbimagenes/

[20] 2013. [Online]. Available: https://www2.eecs.berkeley.edu/Research/Projects/CS/vision/grouping/resources.html

[21] K. Gu, W. Lin, G. Zhai, X. Yang, W. Zhang, and C. W. Chen, "No-reference quality metric of contrast-distorted images based on information maximization," *IEEE Trans. Cybern.*, vol. 47, no. 12, pp. 4559–4565, Jun. 2016.

[22] A. Mittal, R. Soundararajan, and A. C. Bovik, "Making a 'completely blind' image quality analyzer," *IEEE Signal Process. Lett.*, vol. 20, no. 3, pp. 209–212, Mar. 2013.